JCTC Journal of Chemical Theory and Computation

Article

Cite This: J. Chem. Theory Comput. 2019, 15, 6859−6864

pubs.acs.org/JCTC

Large-Scale Phonon Calculations Using the Real-Space Multigrid Method

Jiayong Zhang,[†] Yongqiang Cheng,[‡] Wenchang Lu,[†,§] Emil Briggs,[†] Anibal J. Ramirez-Cuesta,*[,‡] and J. Bernholc[†,§]

[†]Department of Physics, North Carolina State University, Raleigh, North Carolina 27695, United States

[‡]Neutron Scattering Division and [§]Computational Sciences and Engineering Division, Oak Ridge National Laboratory, Oak Ridge, Tennessee 37831, United States

ABSTRACT: Phonons are fundamental to understanding the dynamical and thermal properties of materials. However, first-principles phonon calculations are usually limited to moderate-size systems due to their high computational requirements. We implemented the finite displacement method (FDM) in the highly parallel real-space multigrid (RMG) suite of codes to study phonon properties. RMG scales from desktops to clusters and supercomputers containing thousands of nodes, fully supports graphics processing units (GPUs), including multiple GPUs per node, and is very suitable for large-scale electronic structure calculations. It is used as the core computational kernel to calculate the force constants matrix with FDM. By comparing with other widely used density functional theory packages and experimental data from inelastic neutron scattering, we demonstrate that RMG is very accurate in calculating forces at small displacements from equilibrium positions. The calculated phonon band structures and vibrational spectra for a variety of different systems are in very good agreement with plane-wave-based density functional theory codes, Quantum ESPRESSO, CASTEP and VASP, and these results have been validated comparing with inelastic neutron scattering experimental data measured at the VISION spectrometer at the Spallation Neutron Source.

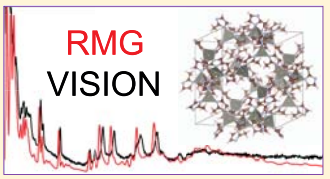

1. INTRODUCTION

Vibrational spectroscopy and phonon band structures play central roles in studies of lattice dynamics and thermal conductivity,[1] vibrational modes are routinely used as fingerprints of chemical species and configuration of adsorbed molecules in solids, etc. In the past few decades, several different methods have been developed to perform phonon calculations, and they have achieved significant success. Due to the continuing development and implementation of theory for phonon calculations within the framework of density functional theory (DFT) as well as the fast development of high-performance computers, researchers are now able to calculate phonon band structures of many materials accurately, at an affordable computational cost and in a reasonable time. However, most procedures are only applicable to systems with a moderate number of atoms, due to the $O(N^4)$ scalability in the first-principles phonon calculations, where N is the number of atoms in the system.

In phonon calculations within DFT, the most challenging and time-consuming part is to build the force constant matrix accurately. There are two common schemes to calculate the force constant matrix. The linear response theory, also called density functional perturbation theory (DFPT),[2,3] is one of the most popular methods. It provides an analytical formalism to calculate the second derivatives of total energy with respect to the atomic coordinates. The DFPT equations can be solved iteratively[2] or variationally.[3] Both methods lead to the same solution and have $O(N^4)$ scalability. The advantage of the DFPT formalism is that the force constant matrix at a specific wave vector can be obtained by calculations using only the primary unit cell. Therefore, this formalism is very efficient for systems with a small primary unit cell. For a large system, DFPT requires vast computational resources due to its scalability and inefficient parallelization.

Another scheme to calculate the force constant matrix is the finite displacement method (FDM), in which the force constant matrix is evaluated by numerically differentiating the Hellmann−Feynman forces on atoms. We will discuss this method in detail in Section 2. Although this method also scales as $O(N^4)$, its natural parallelization over different displacement configurations makes it suitable for large systems. Since the force constants are calculated directly in real space, a supercell is needed when the primary unit cell is so small that the effects from periodic images cannot be neglected. Furthermore, the force constant matrix is only exact at the wave vectors that are commensurate with the supercell. In fact, the force constant matrix at other wave vectors is an interpolation from those at the commensurate wave vectors.[4] FDM is also straightforward to employ in any DFT code that can calculate the forces accurately. In this paper, we implement this method in our real-space multigrid (RMG) suite of DFT codes.[5−7] RMG uses real-space meshes to represent the wave functions, the charge density, and the ionic pseudopotentials. The real-space formulation is advantageous for efficient parallelization via domain decomposition because each processor can be assigned a given region of space. The multigrid technique is used to accelerate the convergence by attenuating errors on

Received: August 8, 2019
Published: October 24, 2019

DOI: 10.1021/acs.jctc.9b00802
J. Chem. Theory Comput. 2019, 15, 6859−6864

successively coarser grids, at which even long-wavelength errors become oscillatory and, thus, are rapidly eliminated. RMG implements both norm-conserving and ultrasoft pseudopotentials.[8] RMG utilizes a mixed programming mode, using a message passing interface (MPI) for parallelization between nodes, while on-node parallelization is handled via OpenMP and C++11 threads. For Nvidia graphics processing unit (GPU) accelerators, Cuda-managed memory is employed for data transfer between central processing units and GPUs, while Cublas and Cusolver libraries are extensively used for GPU acceleration. Due to the extensive parallelization and excellent scaling, RMG is particularly suitable for very large electronic structure calculations and can handle several thousand atoms in a unit cell.

To validate the accuracy of RMG for phonon calculations, RMG results below are compared to those obtained using traditional plane-wave-based DFT codes, Quantum ESPRESSO, VASP, and CASTEP. It is shown that all of the DFT codes generate very similar results that compare equally well with experimental data.

An open-source phonon package for pre- and post-processing of FDM calculations, Phonopy,[1,9] is used to prepare the displacement configurations, extract the force constant matrix, and calculate the phonon properties for all codes except CASTEP.

Molecular dynamics (MD) can also be used to calculate the vibrational spectrum. The phonon density of states is given by the Fourier transform of the velocity−velocity autocorrelation function[10]

$$g(\omega) = \int_{\infty}^{-\infty} \boldsymbol{v}(0)\cdot\boldsymbol{v}(t)\exp(-i\omega t)\mathrm{d}t \tag{1}$$

Since the harmonic approximation is not employed, anharmonic effects are included in the classical molecular dynamics limit. The phonon dispersion can also be obtained from MD by evaluating the lattice Green's function from atomic displacements during the simulation.[11] Recently, MD was employed to study temperature effects on phonon spectra by the temperature-dependent effective potential method (TDEP).[12,13] Similarly to the FDM, TDEP requires MD to be performed in a supercell that is large enough to eliminate periodic image effects. It uses fitting and symmetry analysis to extract the force constant matrix and, optionally, anharmonic higher-order terms in free-energy expansion, from MD data. A disadvantage is that a long-time MD simulation is required to obtain a converged vibrational spectrum. ALAMODE[14] is an open-source package that implements the TDEP method and aims mainly at first-principles calculations for anharmonic systems and evaluation of thermal properties.

Turning to the experiment, vibrational properties can be obtained from diffuse X-ray scattering,[15] infrared spectroscopy,[16] Raman spectroscopy,[17] and inelastic neutron scattering (INS).[10,18] In this paper, we compare the calculated results to INS spectra[18] measured by the VISION spectrometer at the Spallation Neutron Source in the Oak Ridge National Laboratory (ORNL). Compared with other spectroscopy techniques, neutron scattering has advantages of wideband coverage of full phonon spectra with no selection rules to obey and the special capability of capturing hydrogen dynamics because of the proton's large cross-section for neutron scattering. INS spectra measure the intensity variation with energy and the momentum transfer between neutrons and phonons. The INS spectra usually focus on energy transfer. The theoretical intensity spectra can be computed by the OCLIMAX[19,20] software based on vibrational modes obtained from the RMG or other codes.

2. METHODOLOGY

At a finite temperature, all atoms in a crystal or molecule vibrate with small displacements around their equilibrium positions. The system's total energy can be Taylor-expanded in terms of powers of the displacements. The linear term in the Taylor expansion is zero, because at equilibrium, the first derivatives of the total energy, i.e., the forces, are zero on all of the atoms. In the harmonic approximation, all of the powers of displacements larger than two are neglected, and the total energy can be written as

$$E_{\mathrm{tot}}(r) = E_{\mathrm{tot}}(r_0) + \frac{1}{2}\sum_{i\alpha,j\beta}\phi_{i\alpha,j\beta}u^{i\alpha}u^{j\beta} \tag{2}$$

where $u^{i\alpha}$ is the displacement of atom i along the α direction, $\phi_{i\alpha,j\beta}$ is the second derivative of the total energy with respect to atomic positions at equilibrium and is an element of the force constant matrix. Eigenmodes of the dynamical matrix $D_{i\alpha,j\beta}(\mathbf{q})$ can be determined by solving the equation

$$\sum_{j,\beta} D_{i\alpha,j\beta}(\mathbf{q})e_{j\beta} = \omega^2(\mathbf{q})e_{i\alpha} \tag{3}$$

where ω is the frequencies and $e_{i\alpha}$ is the components of the polarization vectors of phonons.

For a crystal with periodic boundary conditions, the dynamical matrix can be represented in the reciprocal space

$$D_{i\alpha,j\beta}(\mathbf{q}) = \frac{1}{\sqrt{m_i m_j}}\sum_{R}\Phi_{i,\alpha,j+R,\beta}\exp[i\mathbf{q}(\mathbf{R}+\boldsymbol{r}_i-\boldsymbol{r}_j)] \tag{4}$$

where $\mathbf{q}$ is the wave vector in the first Brillouin zone, $\mathbf{R}$ is the lattice vector, and $\boldsymbol{r}_i$ and $\boldsymbol{r}_j$ are the atomic positions in the primitive cell.

If the system is in a stable state under the harmonic assumption, the force constant matrix is positive definite and the eigenvalues ω_j^2 are positive. Eigenvalues with negative frequencies usually indicate that the system has not attained the state with the minimum energy, i.e., the structure is dynamically unstable, and could further indicate the possibility of phase transition[1] or certain physical rules are not satisfied due to numerical errors (e.g., the acoustic sum rule to be discussed below), or even that the harmonic approximation is not applicable, in which case the system can alternatively be analyzed using the MD method.[21]

Focusing on the FDM, we evaluate the interatomic force constant by using the following formula

$$\phi_{i\alpha,j\beta} = \frac{\partial^2 E}{\partial r_{i\alpha}\partial r_{j\beta}} = \frac{\partial F_{j\beta}}{\partial r_{i\alpha}} = \frac{F_{j\beta}(r_{i\alpha}+u_{i\alpha}) - F_{j\beta}(r_{i\alpha}-u_{i\alpha})}{2u_{i\alpha}} \tag{5}$$

where $F_{j\beta}$ is the force on atom j along the β direction after a small displacement $u_{i\alpha}$ of atom i, which can be accurately and easily calculated by the Hellmann−Feynman theorem as shown in eq 6, where H is the Hamiltonian operator and ψ is the wavefunction of H.

DOI: 10.1021/acs.jctc.9b00802
J. Chem. Theory Comput. 2019, 15, 6859−6864

$$F_{j\beta} = -\frac{\partial E}{\partial u_{j\beta}} = -\left\langle \psi \left| \frac{\partial H}{\partial u_{j\beta}} \right| \psi \right\rangle \tag{6}$$

Alternatively, one may directly calculate force constants from the second derivative of the total energy, without calculating forces explicitly. However, the energy-based method will require more computational cost as it needs more displacement configurations and higher accuracy in DFT calculations (due to the second derivatives) than the force-based method in eq 5.

The advantage of the FDM can be clearly seen from the above formula. Without a new algorithm, any DFT code can be used to calculate the force constant matrix by evaluating the forces at appropriate displacement configurations. In the real space, the interatomic force constants decay quickly to zero with distance. In our implementation, a force constant is set to zero when the distance between two atoms is larger than the cutoff radius R_C. R_C, thus, varies for different systems and also depends on the desired accuracy. For a system with periodic boundary conditions, the primitive unit cell may not be large enough to calculate all of the non-negligible force constants with a finite displacement configuration. In this case, one must choose a supercell, which will contain the sphere described by the cutoff radius.

For a system with a primitive unit cell containing N atoms, we need to calculate forces in a supercell by perturbing each atom in the primitive unit cell. For each atom, two displacements are required to get accurate force constants. In total, $6N$ different displacement configurations need to be considered to extract the force constant matrix. The resulting matrix in the real space has dimensions $3N \times 3NM$, where M is the number of primitive unit cells in the supercell.

Symmetry operation can be used to reduce the number of displacement configurations. If the atoms i, j transform to their equivalent atoms is, js under a symmetry operation S, the force constants between these two pairs of atoms satisfy the following relation[22]

$$\Phi_{is,js} = S \cdot \Phi_{i,j} \cdot S^{-1} \tag{7}$$

Mathematically, the force constant matrix should satisfy two rules. The first is the symmetry of the matrix

$$\Phi_{i\alpha,j\beta} = \Phi_{j\beta,i\alpha} \tag{8}$$

because the second derivative operators commute in eq 5. The second is the acoustic sum rule (ASR)

$$\sum_{i,j} \Phi_{i\alpha,j\beta} = 0 \tag{9}$$

which is the result of translational invariance.

In calculations, the interatomic force constants are extracted from total energy and force calculations with different atomic displacements and are set to zero when the distance between two atoms is larger than the cutoff radius R_C. Therefore, these two rules are broken due to numerical errors. The symmetry rule can be restored by averaging the off-diagonal elements. The ASR can be imposed in three possible ways. The first one is to subtract the corresponding fraction of the sum residuals from the diagonal elements $\Phi_{i\alpha,i\beta}$ only, the second one is to adjust each nonzero element by the same amount, and the third one is to adjust the nonzero elements proportionally to their magnitudes. We will use the first option because it usually outperforms the other two options.[23] When the ASR is imposed, the symmetry rule may be broken again. Therefore, we iteratively impose these two rules until both conditions are satisfied.

From eq 5, the most time-consuming parts of the FDM phonon calculations are the self-consistent calculations for all atomic displacement configurations. An interface code between Phonopy and RMG has been developed. The workflow is as follows. First, the atomic structure of the system is optimized with RMG using the primary unit cell. Second, a supercell is determined by the cutoff radius of the force constants. Phonopy is used to set up the displacement configurations by taking into consideration the crystal symmetry of the system. Third, the forces on atoms at each displacement configuration are calculated by RMG. Fourth, the force constant matrix is constructed by Phonopy and self-consistently adjusted to satisfy the two rules discussed above. The phonon band structure and the vibrational spectrum are then calculated. For Quantum ESPRESSO and VASP, the interfaces to Phonopy already exist and have been used in the same workflow.

A different way to extract the force constant matrix is by performing long-enough MD simulations in NVT/NVE ensembles. The displacement−force dataset from the MD trajectories is used to extract the force constant matrix by the open-source package ALAMODE. The anharmonic effects can also be included if needed. We have also written an interface between ALAMODE and RMG. The workflow is the same as RMG-Phonopy's in the first step. Then, a sufficiently large supercell is built with the optimized structure and MD simulations are performed by RMG in NVT/NVE ensembles. The displacement−force dataset extracted from the MD trajectories is used to fit the effective force constant matrix ($\tilde{\mathbf{\Phi}}$, $3N \times 3N$) by ALAMODE via minimizing the sum of differences between the fitted ($\tilde{\mathbf{F}}(m) = \mathbf{U}(m)\mathbf{\Phi}$, $1 \times 3N$) and the real forces ($\mathbf{F}(m)$, $1 \times 3N$) for all displacement configurations M,[14] where $\mathbf{U}(m)$ ($1 \times 3N$) is the vector composed of the mth atomic displacements

$$\tilde{\mathbf{\Phi}} = \arg\min_{\mathbf{\Phi}} \sum_{m=1}^{M} \| \mathbf{U}(m)\mathbf{\Phi} - \mathbf{F}(m) \|^2. \tag{10}$$

3. RESULTS AND DISCUSSION

Phonon calculations have been performed on four systems with increasingly larger unit cell sizes: silicon (Si), zirconium(II) hydride (ZrH_2), carbazole ($C_{48}H_{36}N_4$), and zeolitic imidazolate frameworks (ZIF)-8 ($C_{96}H_{120}N_{48}Zn_{12}$). Since the force constants are calculated by finite displacements in our implementation, highly accurate total energy and force calculations need to be performed. To validate the accuracy of the RMG, the calculated phonon band structures and/or vibrational spectra are compared with the results obtained using other DFT packages, such as Quantum ESPRESSO (QE),[24] VASP,[25,26] and CASTEP.[27] Different from the RMG method, in which the wave functions are represented on a real-space grid, the other three packages use plane waves to represent the wave functions. In the examples discussed below, for all of the supercell calculations, the small displacements are set to 0.01 Å and only the Γ point is used for Brillouin sampling, because the supercell must be large enough to eliminate the periodic image effect in the force constants.

DOI: 10.1021/acs.jctc.9b00802
J. Chem. Theory Comput. 2019, 15, 6859−6864

3.1. Silicon. Silicon crystallizes in the diamond structure and has very high symmetry. Its primary unit cell has only two atoms, and its physical properties are well known. Therefore, silicon is a very good candidate to benchmark the accuracy of phonon calculations with RMG. Here, we use a supercell consisting of 2 × 2 × 2 cubic cells to perform the FDM calculations. Figure 1 shows the phonon band structures

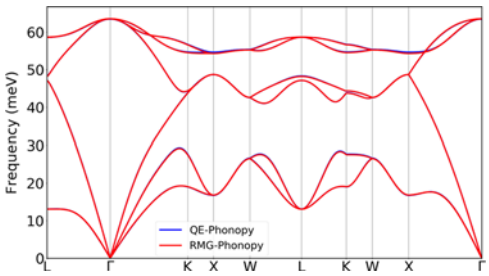

Figure 1. Phonon dispersions of crystalline silicon calculated by QE-Phonopy (blue) and RMG-Phonopy (red). The results are nearly identical, and the two curves fall on top of each other.

calculated with RMG-Phonopy and QE-Phonopy. The same norm-conserving pseudopotentials were used for both RMG and QE. The real-space grid spacing was 0.17 Å, and the plane-wave cutoff was 40.0 Ry. The perfect agreement between the two sets of results shows that the real-space method (RMG) performs as accurately as the plane-wave based method.

3.2. Zirconium(II) Hydride. Zirconium alloys with hydrogen are of great interest to researchers for their promising potential to store hydrogen atoms as well as their applications in nuclear reactors and neutron scattering science.[28,29] Zirconium hydride has different crystalline phases depending on hydrogen concentration. At a very low hydrogen concentration, the most stable structure is the metallic phase α-Zirconium with the hcp structure. As the hydrogen concentration increases, its crystal structure transitions to the face-centered cubic (δ-Zr) and then the face-centered tetragonal (ε-Zr). Here, we focus on the high-concentration ε-Zr phase, ZrH_2, which contains the most H. It has the body-centered tetragonal (bct) structure with the space group of I4/mmm and c/a = 1.2639.

The supercell for the displacement configurations contains 3 × 3 × 2 primary unit cells and 108 atoms. The valence electron configuration of Zr was set to 5s4d.

Figure 2 shows the phonon band structures calculated by RMG and QE, which are also in excellent agreement with each other. The grid spacing of 0.111 Å is used in RMG, and the plane-wave cutoff of 80 Ry for wave functions is used in QE.

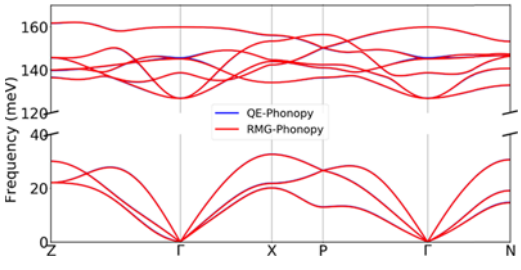

Figure 2. Phonon dispersions of ZrH_2 calculated by RMG-Phonopy (red) and QE-Phonopy (blue).

Figure 3 shows the calculated vibrational spectra compared to the results of neutron scattering experiments performed with

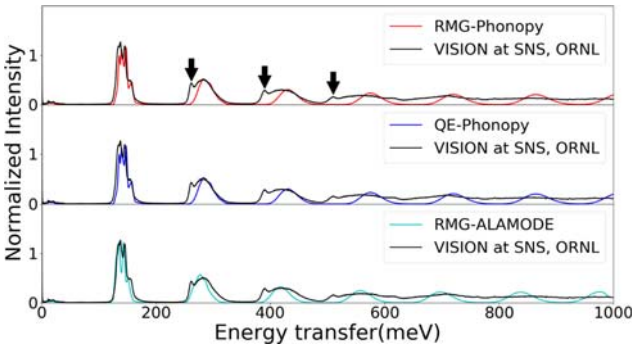

Figure 3. Vibrational spectra from RMG-Phonopy (red), QE-Phonopy (blue), RMG-ALAMODE (cyan), and VISION's experimental data (black) at 5 K for ZrH_2. Overtone peaks, which correspond to multiple phonon scattering events, are generated by the convolution of the DFT-calculated fundamental peaks by the OCLIMAX software. The peaks below 200 meV are from one-phonon scattering events, while those above 200 meV result from the scattering of two or more phonons. Extra sharp peaks marked by black arrows might be due to anharmonic effects.

VISION. The intensities from theory are normalized to the experimental spectrum. The FDM results from RMG and QE are very similar and agree equally well with the experimental data. The calculated one-phonon scattering spectra around 150 meV are in good agreement with the experimental data, while there are some discrepancies between the theory and experiment when two or more phonons are emitted. For the sharp peaks marked by arrows in the experimental data, the significantly decreasing interpeak spacing strongly suggests anharmonic effects. Kolesnikov et al. attributed it to bound-state multiphonons.[30] Since our current calculations are based on the harmonic approximation, we are not able to include anharmonicity in the multiphonon scattering spectrum.

The bottom panel in Figure 3 shows the phonon spectrum computed from molecular dynamics using RMG and ALAMODE. There is a slight improvement over the RMG-Phonopy results, confirming that the extraction of force constants from molecular dynamics is practical for these systems. While thermal and anharmonic effects are quite small for these materials, the RMG-ALAMODE procedure can also be used for phases that would not be stable at 0 K and would, thus, exhibit negative phonon modes if the FDM was used.

3.3. Carbazole. Carbazole is an aromatic heterocyclic organic compound. It consists of two six-membered benzene rings and one five-membered nitrogen-containing ring. Polycarbazole can potentially be used as a blue light emitter.[31] In crystalline carbazole, four carbazole molecules form an orthorhombic structure with lattice constants of 5.725 × 7.772 × 19.182 $Å^3$.

In our calculations, the atomic structure is optimized using a Brillouin Zone sampling mesh of 3 × 3 × 1, which reduces to four irreducible k-points. The maximum residual force is set to be 0.05 mHa/Bohr so that the force constants can be calculated accurately by FDM. The supercell for displacement configurations includes 3 × 3 × 1 primitive unit cells with 792 atoms in total. The same norm-conserving pseudopotentials with the Perdew−Burke−Ernzerhof (PBE) exchange-correlation functional are used in QE and RMG, while projector-

DOI: 10.1021/acs.jctc.9b00802
J. Chem. Theory Comput. 2019, 15, 6859−6864

augmented waves[26,32] and norm-conserving pseudopotentials are used in VASP and CASTEP, respectively. The grid spacing in RMG is 0.159 Å, while the plane-wave cutoffs are 40 Ry, 800 eV, and 800 eV in QE, VASP, and CASTEP, respectively.

In Figure 4, we show normalized intensity comparisons between different codes and VISION's measurements. Overall,

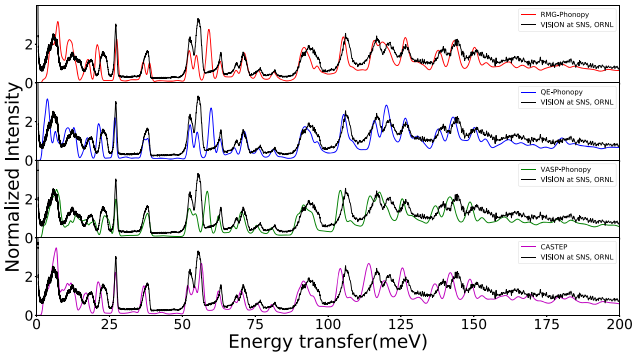

Figure 4. Normalized intensity comparisons between RMG-Phonopy (red), QE-Phonopy (blue), VASP-Phonopy (green), CASTEP (magenta), and experimental data (black) at 5 K for carbazole.

there is a good agreement between all of the different codes and the experiment, although some discrepancies exist at various energy ranges. At 35 meV, VASP and CASTEP show one peak, while RMG and QE show two peaks with a small splitting. At 55 meV, the results from RMG and QE agree well with each other and also with VASP but have a few meV shift compared to the results from CASTEP. These subtle differences may result from different implementations used in different codes, e.g., in filtering pseudopotentials, the numerical approximations for the Laplacian and gradient operators, etc.

3.4. ZIF-8. Zeolitic imidazolate frameworks (ZIFs) are metal−organic frameworks that are topologically isomorphic with zeolites. They have wide-ranging applications in carbon capture due to their robust porosity, resistance to thermal changes, and chemical stability. Among all of the ZIFs, ZIF-8 $C_{96}H_{120}N_{48}Zn_{12}$ has been further investigated for applications in supercapacitors and as a catalyst, e.g., to reduce CO_2.[33]

The crystal structure of the ZIF-8 is a simple cubic with I-43m space group symmetry. There are 276 atoms in the unit cell. The lattice constant is 16.992 Å and the Γ point is sufficient to sample the Brillouin Zone. For the scalar-relativistic Zn pseudopotential, 3d and 4s electrons were treated as valence. The PBE functional is used, and the forces are converged until the maximum residual force is smaller than 0.1 mHa/Bohr. The RMG grid spacing was 0.132 Å, and the plane-wave cutoffs were 80 Ry.

In Figure 5, the vibrational spectra calculated by RMG and QE are shown together with VISION's experimental results. The calculated spectra agree with each other very well except for discrepancies at very low energies. The simulated results are also in very good agreement with the experimental results.

4. SUMMARY AND CONCLUSIONS

In summary, we have shown that the open-source real-space multigrid (RMG) suite of codes can provide accurate total energies and forces that can be used to obtain phonon spectra in very good agreement with plane-wave-based codes and experiment. An interface to Phonopy open-source phonon calculations package has been developed, which allows for easy

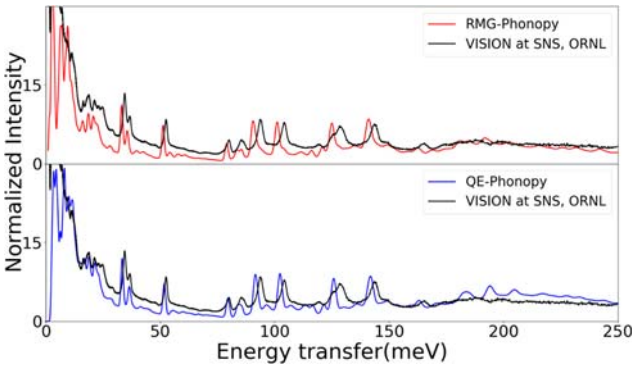

Figure 5. Comparisons of low-frequency vibrational intensities among RMG-Phonopy (red), QE-Phonopy (blue), and experimental data (black) at 5 K for ZIF-8.

calculation of vibrational properties of a large range of materials using RMG as the DFT computational kernel. We have also developed an RMG interface to the ALAMODE software for extraction of force constants from ab initio molecular dynamics via the temperature-dependent effective potential method to facilitate extraction of vibrational properties at finite temperatures and for anharmonic crystals. Since RMG is highly scalable on supercomputers and clusters and also offers scalable GPU support, it can be used in the future for very large-scale phonon calculations.

AUTHOR INFORMATION

ORCID

Yongqiang Cheng: 0000-0002-3263-4812
Anibal J. Ramirez-Cuesta: 0000-0003-1231-0068
J. Bernholc: 0000-0002-9981-8851

Notes

The authors declare no competing financial interest.

ACKNOWLEDGMENTS

Neutron scattering experiments were conducted at ORNL's Spallation Neutron Source, which is supported by the Scientific User Facilities Division, Office of Basic Energy Sciences (BES), U.S. Department of Energy (DOE), under Contract No. DE-AC0500OR22725 with UT Battelle, LLC. The computing resources were made available through the VirtuES and the ICEMAN projects, funded by Laboratory Directed Research and Development program at ORNL. The development of the RMG code was funded by NSF grant OAC-1740309. Supercomputer time was provided by NSF grant ACI-1615114 at the National Center for Supercomputing Applications (NSF OCI-0725070 and ACI-1238993).

REFERENCES

(1) Togo, A.; Tanaka, I. First Principles Phonon Calculations in Materials Science. *Scr. Mater.* **2015**, *108*, 1−5.

(2) Baroni, S.; de Gironcoli, S.; Dal Corso, A.; Giannozzi, P. Phonons and Related Crystal Properties from Density-Functional Perturbation Theory. *Rev. Mod. Phys.* **2001**, *73*, No. 515.

(3) Gonze, X.; Lee, C. Dynamical Matrices, Born Effective Charges, Dielectric Permittivity Tensors, and Interatomic Force Constants from Density-Functional Perturbation Theory. *Phys. Rev. B* **1997**, *55*, No. 10355.

(4) Wang, Y.; Shang, S.-L.; Fang, H.; Liu, Z.-K.; Chen, L.-Q. First-Principles Calculations of Lattice Dynamics and Thermal Properties of Polar Solids. *npj Comput. Mater.* **2016**, *2*, No. 16006.

DOI: 10.1021/acs.jctc.9b00802
J. Chem. Theory Comput. 2019, 15, 6859−6864

(5) Briggs, E. L.; Sullivan, D. J.; Bernholc, J. Real-Space Multigrid-Based Approach to Large-Scale Electronic Structure Calculations. *Phys. Rev. B* **1996**, *54*, No. 14362.
(6) Hodak, M.; Wang, S.; Lu, W.; Bernholc, J. Implementation of Ultrasoft Pseudopotentials in Large-Scale Grid-Based Electronic Structure Calculations. *Phys. Rev. B* **2007**, *76*, No. 085108.
(7) RMG Website. http://www.rmgdft.org/ (accessed July 9, 2019).
(8) Vanderbilt, D. Soft Self-Consistent Pseudopotentials in a Generalized Eigenvalue Formalism. *Phys. Rev. B* **1990**, *41*, No. 7892.
(9) Togo, A. Phonopy Website. https://atztogo.github.io/phonopy/ (accessed January 7, 2019).
(10) Mitchell, P. C.; Parker, S. F.; Ramirez-Cuesta, A. J.; Tomkinson, J. *Vibrational Spectroscopy with Neutrons: With Applications in Chemistry, Biology, Materials Science and Catalysis*; World Scientific, 2005.
(11) Kong, L. T. Phonon Dispersion Measured Directly from Molecular Dynamics Simulations. *Comput. Phys. Commun.* **2011**, *182*, 2201−2207.
(12) Hellman, O.; Abrikosov, I. A. Temperature-Dependent Effective Third-Order Interatomic Force Constants from First Principles. *Phys. Rev. B* **2013**, *88*, No. 144301.
(13) Hellman, O.; Abrikosov, I. A.; Simak, S. I. Lattice Dynamics of Anharmonic Solids from First Principles. *Phys. Rev. B* **2011**, *84*, No. 180301.
(14) Tadano, T.; Gohda, Y.; Tsuneyuki, S. Anharmonic Force Constants Extracted from First-Principles Molecular Dynamics: Applications to Heat Transfer Simulations. *J. Phys.: Condens. Matter* **2014**, *26*, No. 225402.
(15) Dederichs, P. H. The Theory of Diffuse X-Ray Scattering and Its Application to the Study of Point Defects and Their Clusters. *J. Phys. F: Met. Phys.* **1973**, *3*, 471.
(16) Stuart, B. Infrared Spectroscopy. In *Kirk−Othmer Encyclopedia of Chemical Technology*; American Cancer Society, 2015; pp 1−18.
(17) Long, D. A. *Raman Spectroscopy*; McGraw-Hill: New York, 1977.
(18) Parker, S. F.; Ramirez-Cuesta, A. J.; Daemen, L. Vibrational Spectroscopy with Neutrons: Recent Developments. *Spectrochim. Acta, Part A* **2018**, *190*, 518−523.
(19) Ramirez-Cuesta, A. J. ACLIMAX 4.0.1, The New Version of the Software for Analyzing and Interpreting INS Spectra. *Comput. Phys. Commun.* **2004**, *157*, 226−238.
(20) Cheng, Y. Q.; Daemen, L. L.; Kolesnikov, A. I.; Ramirez-Cuesta, A. J. Simulation of Inelastic Neutron Scattering Spectra Using OCLIMAX. *J. Chem. Theory Comput.* **2019**, *15*, 1974−1982.
(21) Kathmann, S. M.; Mundy, C. J.; Schenter, G. K.; Autrey, T.; Aeberhard, P. C.; David, B.; Jones, M. O.; Ramirez-Cuesta, T. Understanding Vibrational Anharmonicity and Phonon Dispersion in Solid Ammonia Borane. *J. Phys. Chem. C* **2012**, *116*, 5926−5931.
(22) Alfè, D. PHON: A Program to Calculate Phonons Using the Small Displacement Method. *Comput. Phys. Commun.* **2009**, *180*, 2622−2633.
(23) Ackland, G. J.; Warren, M. C.; Clark, S. J. Practical Methods in Ab Initio Lattice Dynamics. *J. Phys.: Condens. Matter* **1997**, *9*, 7861.
(24) Giannozzi, P.; Andreussi, O.; Brumme, T.; Bunau, O.; Nardelli, M. B.; Calandra, M.; Car, R.; Cavazzoni, C.; Ceresoli, D.; Cococcioni, M.; et al. Advanced Capabilities for Materials Modelling with Quantum ESPRESSO. *J. Phys.: Condens. Matter* **2017**, *29*, No. 465901.
(25) Kresse, G.; Furthmüller, J. Efficiency of Ab-Initio Total Energy Calculations for Metals and Semiconductors Using a Plane-Wave Basis Set. *Comput. Mater. Sci.* **1996**, *6*, 15−50.
(26) Kresse, G.; Joubert, D. From Ultrasoft Pseudopotentials to the Projector Augmented-Wave Method. *Phys. Rev. B* **1999**, *59*, No. 1758.
(27) Clark, S. J.; Segall, M. D.; Pickard, C. J.; Hasnip, P. J.; Probert, M. I. J.; Refson, K.; Payne, M. C. First Principles Methods Using CASTEP. *Z. Krist. − Cryst. Mater.* **2009**, *220*, 567−570.
(28) Blomqvist, J.; Olofsson, J.; Alvarez, A.-M.; Bjerkén, C. Structure and Thermodynamical Properties of Zirconium Hydrides from First-Principle. *15th International Conference on Environmental Degradation of Materials in Nuclear Power Systems-Water Reactors*; Busby, J. T., Ilevbare, G., Andresen, P. L., Eds.; John Wiley & Sons, Inc., 2012; pp 671−679.
(29) Chattaraj, D.; Parida, S. C.; Dash, S.; Majumder, C. First Principles Study of the ZrX_2 (X = H, D and T) Compounds. *Int. J. Hydrogen Energy* **2014**, *39*, 9681−9689.
(30) Kolesnikov, A. I.; Bashkin, I. O.; Belushkin, A. V.; Ponyatovsky, E. G.; Prager, M. Inelastic Neutron Scattering Study of Ordered Gamma -ZrH. *J. Phys.: Condens. Matter* **1994**, *6*, 8989.
(31) Grimsdale, A. C.; Jacob, J. Polymer-Based LEDs and Solar Cells. In *Reference Module in Materials Science and Materials Engineering*; Elsevier, 2016.
(32) Blöchl, P. E. Projector Augmented-Wave Method. *Phys. Rev. B* **1994**, *50*, No. 17953.
(33) Wang, Y.; Hou, P.; Wang, Z.; Kang, P. Zinc Imidazolate Metal−Organic Frameworks (ZIF-8) for Electrochemical Reduction of CO_2 to CO. *ChemPhysChem* **2017**, *18*, 3142−3147.

DOI: 10.1021/acs.jctc.9b00802
J. Chem. Theory Comput. 2019, 15, 6859−6864